Insight in the behavior of bipolar membrane equipped carbon dioxide electrolyzers at low electrolyte flowrates

Insight in the Behavior of Bipolar Membrane Equipped Carbon Dioxide Electrolyzers at Low Electrolyte Flowrates

Bert De Mot[1], Jonas Hereijgers[1], Nick Daems[1, 2], Tom Breugelmans[1, 2, *]

[1] Research group Applied Electrochemistry & Catalysis, University of Antwerp, Universiteitsplein 1, 2610 Wilrijk, Belgium

[2] Separation & Conversion Technologies, VITO, Boeretang 200, 2400 Mol, Belgium.

*Corresponding author: tom.breugelmans@uantwerpen.be

ABSTRACT: Electrochemical CO_2 reduction is a promising carbon capture and utilization technique, which is urgently required to prevent earth's global warming. Extensive research on catalyst improvement, reactor engineering and electrode development has been performed in order to develop an industrially scalable system. However, despite the great process that has been made, there is still a lack of understanding in the fundamental behavior of the electrolyzers. To reduce this gap, we have investigated the influence of product selectivity and current density on the pH of the catholyte in bipolar membrane electrolyzers. More specifically we have found that, by targeting formate production, consumption of bulk bicarbonate occurs, which can cause a pH drop of the catholyte. Especially at low catholyte flowrates and high partial current densities, it was shown that this phenomenon can negatively affect the cells performance due to a high concentration of protons in combination with a high residence time of the catholyte. By implementing these fundamental findings, we were able to operate the electrolyzer under acidic conditions, without affecting the electrolyzers performance, allowing us to produce formic acid rather than formate which has not yet been achieved in bipolar membrane based electrolyzers. Under optimal conditions, we achieved a product stream with a formic acid/formate ratio of 0.67 and a combined concentration of 34 g/l, a partial current density of 152 mA/ cm^2 and a cell voltage of 6V.

INTRODUCTION

In the past decade, carbon capture and utilization (CCU) has gained considerable interest from academia and industry as a complimentary measure to reduce carbon dioxide (CO_2) emissions.[1–4] A promising CCU technology is the electrochemical reduction of CO_2 (eCO2R) to value-added products.[5,6] Over the years, a wide variety of electrocatalysts have been assessed on their reactivity towards eCO2R. Overall it was found that three groups of products can be acquired: formate/formic acid, carbon monoxide [7–9] and a variety of C1/C2 products [10–12]. From these products, formate/formic acid is assumed to be one of the most promising products for industrial scale CO_2 electrolysis [13] and this mainly due to (1) the two electron-transfer which translates into a low energy consumption, (2) the broad range of applications in the chemical, food and agriculture industry[14] and (3) its potential as an energy carrier in direct formate fuel cells.[15]

Therefore extensive research has been performed in order to develop formate producing electrocatalysts with high performance (e.g. high stability, selectivity, current density), such as: Sn[16,17], SnO$_2$[18–20], Bi[21,22], In[23,24], metal organic frameworks[25–27] and Pb[28–30]. However, most of these catalyst screenings were performed in H-cell's, in which the reaction rate is limited by the low solubility and diffusion of CO_2 in aqueous solutions, typically resulting in reaction rates not greater than 40 mA/cm^2.[31] As it is shown that CO_2 electroreduction needs to be performed at current densities of at least 100 mA/cm^2 to be industrially viable[32,33], researchers have shifted their focus towards reactor engineering to increase the CO_2 mass transfer and thereby the reaction rate while maintaining the good performance of the catalyst.[34]

The major development in electrochemical CO_2 reactor engineering is the implementation of gas diffusion electrodes (GDE), which allow gaseous CO_2 to be fed directly into the cell.[35] As a result, the diffusion length of dissolved CO_2 towards the catalyst surface is heavily reduced and thereby current densities well above 100 mA/cm^2 can be achieved [36]. Since its first implementation, additional research has been performed on the optimization of these GDE based electrolyzers, mainly by studying the catalyst deposition

method[37,38], binder material[39], catalyst loading[40], GDE flooding [41,42] and reactor configuration (flow-by versus zero-gap).[43,44]

In these GDE based electrolyzers an ion exchange membrane is often used to separate the anode from the cathode compartment. Three types of membranes are described in literature: cation exchange membrane (CEM)[31], anion exchange membrane (AEM)[45] and bipolar membrane (BPM).[46–48] Out of these three the CEMs are most commonly used due to the extensive knowledge gained from their use in fuel cells and water electrolyzers[49]. However the use of CEMs in CO_2 electrolyzers, where the anolyte is often a strong alkaline solution, promotes the migration of metal ions (e.g. potassium) from the anolyte which cause salt deposition problems on the cathode side.[50] Additionally, while AEMs show promising results in CO and hydrocarbon producing electrolyzers, it cannot be used in an electrolyzer targeting formate since it is shown that due to the anionic characteristic of the product, formate crossover towards the anolyte occurs. In the anolyte the formate will be diluted, increasing the downstream separation cost and partly reoxidized to CO_2 at the anode decreasing the efficiency of the electrolyze. . Lastly, AEMs also allow crossover of carbonate to the anode, which results in a high net loss of unreacted CO_2 (also known as CO_2 pumping).[51]

The third alternative are BPMs, this type of membrane is constructed of a cation exchange layer and an anion exchange layer, which are pressed together. At the center junction of the membrane (the interface where the two layers connect) a catalyst is deposited (e.g. $Al(OH)_3$). When current is applied through the membrane, the catalyst at the junction will promote the potential driven dissociation of water molecules into protons and hydroxyl ions. The potential will initiate the migration of these protons through the cation exchange layer towards the cathode and the migration of the hydroxyl ions through the anion exchange layer towards the anode. To prevent the dehydration of the centre junction due to the water splitting reaction, water has to diffuse from either one of the electrolyte compartments to the centre of the membrane to prevent its dehydration.[52] Recently, BPMs have gained interest from electrochemists due to their combined ability to prevent crossover and stabilize the pH in the electrolyte compartments.[53,54] A more detailed understanding of the working mechanism of BPMs in eCO2R electrolyzer is provided by D. A. Vermaas et al.[47] A good example of how these membranes can be used to upscale the eCO2R process was described by Chen et al.[55] Nevertheless, there are still certain pitfalls which could limit the widespread use of these BPM electrolyzers. First the extra energy required for the water dissociation and the high ohmic resistance of the two exchange layers increase the total cell voltage, which negatively affects the energy efficiency of the system. To this end, research on BPMs in this field has recently focused on reducing their resistance in order to diminish the required cell voltage. In this respect, 3D electro spun junctions[56] and decreased exchange layer thickness have proven to be promising paths towards BPMs with reduced resistances.[57] A second pitfall in BPMs is the acidity of the cation exchange layer, promoting hydrogen evolution (HER) at the cathode. Changing the acidity of the cation layer can slightly reduce this negative effect[58], but more effective is the use of a buffer solution as electrolyte between the membrane and the cathode. The latter allowed Chen et al. to construct a reactor system with exquisite performance and scaling possibilities, however at the cost of diluted formate concentrations and increased downstream processing cost.[55]

Overall it is clear that BPMs have great potential in eCO2R electrolyzers, yet additional research is required to understand their overall functioning. Therefore, in this manuscript we will discuss how the behavior of (ionic) species can heavily influence the catholyte pH and consequently the electrolyzer performance. More specifically it will be shown that, at high partial current densities towards formate, a consumption of bulk bicarbonate occurs. Thereby the catholyte buffering capacities can be nullified which results in a decrease of bulk catholyte pH. In current BPM research, this effect has not yet been observed, presumably due to the masking effect of high catholyte flowrates, which increases the downstream processing costs (low formate concentration). Therefore, the effect of catholyte flowrate on the pH was investigated, as well as the influence of the pH drop on the electrolyzer performance in an attempt to address this issue.

EXPERIMENTAL

Chemicals

Tin (IV) oxide nanopowder (< 100nm, >99%), Ag nanopowder (< 100nm, >99.5%) and Nafion perfluorinated resin solution (5 wt%) were purchased from Sigma-Aldrich (Belgium). Isopropyl alcohol (99.8%, electronic use), potassium hydroxide (p.a. grade) and potassium bicarbonate (99.5%) were purchased from Chemlab (Belgium). Sigracet 39 BB GDL was purchased from Ion Power (Germany). Ultrapure water was prepared in the laboratory (Milli-Q gradient, Millipore, USA). The bipolar membrane (type FBM) was purchased from Fumasep (Germany) while the cation exchange membrane (Nafion 117) was purchased from Fuel Cell Store (USA). Ni foam anode was purchased from Nanografi (Turkey). CO2 (99.998 %) and Ar (99.999 %) were purchased from Nippon (Belgium).

GDE preparation

The GDEs used in the experiments were prepared by ink spraying. For a GDE with a geometrical surface of 16 cm^2, 100 mg of nanoparticles were mixed with a 5 w% Nafion solution to obtain a 85/15 mixture. Next, 3 ml of isopropyl alcohol and 3 ml of water was added after which the ink solution was thoroughly sonicated for 30 minutes. The GDLs were spray-coated using an airbrush with argon as carrier gas. During the spraying procedure, the GDL was heated with a hotplate to 60 °C to promote the drying of the ink. The electrodes were weighted before and after the spray coating procedure to determine the final loading of catalyst which was 2.5 mg/cm^2.

<u>Sample analysis</u>

Both gaseous and liquid samples were taken 15 minutes after the reactor reached steady-state to ensure the absence of any start-up phenomena. The gaseous products were analyzed using a GC (Shimadzu 2014, Japan) in which a ShinCarbon St 100/120 2mx1mm column (Restek, USA) was installed. Helium gas (10 ml/min) was used as carrier and the temperature of the column was set at 40°C for 180 seconds. After the initial stage the column's temperature was raised by 40°C/min to 250°C. Detection of the products was done by a thermal conductivity detector at 280°C. For the correct FE calculation of the gaseous products it is required to measure the outlet gas flowrate of the system, as it has been demonstrated by M. Ma et al. that this can vary strongly from the inlet gas flowrate due to CO_2 neutralization.[51] Therefore a gas flow meter (ProFlow 6000, Restek) was used to correctly determine the gas flowrates and calculate the FE's for these products.

A HPLC system (Alliance 2695, Waters, USA) combined with a PDA detector (2996, Waters, at 210 nm) and a packed column (IC-Pak, Waters, USA) was used to analyze the concentration of the liquid products in the catholyte. A perchloric acid solution (0.1%) was used as mobile phase. Depending on the concentration of the products in the catholyte the samples were diluted 1 or 10 times. A pH meter (Consort C860 / SI Analytics pH electrode BlueLine) was used to measure the bulk pH of the catholyte samples exiting the electrolyzer. To minimize the void volume of the system, the exiting catholyte was sampled directly at the outlet of the electrolyzer. Catholyte samples were taken using conical sample tubes, thereby a sample volume of 0.5 – 1 ml, corresponding to a sampling time of 10-100 s depending on the flowrate is sufficient for accurate pH analysis.

<u>Electrolyzer set-up</u>

A detailed description of the custom made electrolyzer can be found in previous reports.[41] Flow channels are milled out of impervious graphite (Fuel Cell Store, USA) and the catholyte spacer was fabricated in PMMA. The thickness of the spacer was reduced to 1 mm to minimize the ohmic resistance of the catholyte and to limit the void volume of the cell to 1.5 ml. The GDE was pressed against the graphite flow channel to allow electrical contact with the potentiostat (Metrohm, Multi Autolab M204, 10A booster module). On the anode side Ni foam was used as counter electrode and was pressed directly against the membrane to limit the ohmic resistance. Aluminium endplates, EPDM gaskets and M6 bolts were used to assemble and seal the electrolyzer.
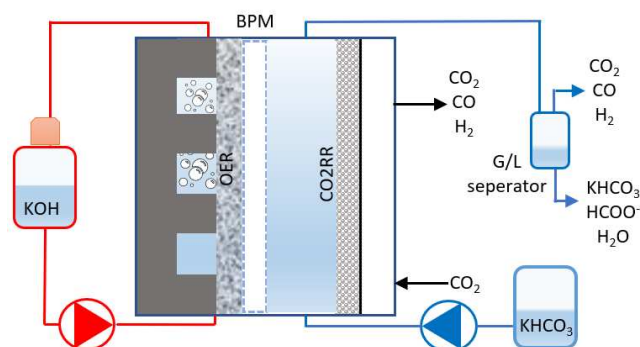

Figure 1. schematic presentation of the experimental set-up of the eCO2R electrolyzer used in the manuscript.

The experimental set-up is graphically visualized on figure 1. A peristaltic pump (Ismatec, Reglo ICC) was used to provide the flow of potassium hydroxide (20 ml/min) to the anode compartment while a HPLC pump (Watrex, P102) was used to control the flow of the catholyte. The flow of CO_2 was set at 200 ml/min with a mass flow controller (Brooks instruments, GF040). The liquid/gas mixture exiting the electrolyzer was separated using a custom-made gas/liquid separator after which the products were analyzed. At the catholyte side, the liquid is fed in a single pass. The temperature of the system was maintained at 60°C throughout the experiments. The performance of the reactor was assessed by chrono potentiometric experiments at increasing current densities, at each setpoint the current is applied for 15 minutes to stabilize the system after which product samples were taken and subsequently the current was increased to the next setpoint. The data is represented as a partial polarization curve, taking Faradaic efficiencies into account. Experiments were repeated at least three times with new GDEs, membranes, and assembly, to determine error margins on the experiments.

RESULTS & DISCUSSION

<u>Theoretical background</u>

To understand the transport behavior of (ionic) species in BPM equipped electrolyzers and to unravel how they influence the catholyte pH, all the reactions that can occur inside the catholyte compartment are assessed (Eqs. 1-8). As the focus of this manuscript lies on the reduction of CO_2, only the reactions in the cathodic compartment will be discussed. These reactions can be divided in two groups: (1) the reactions occurring at the GDE interface:

$$CO_2 + H_2O + 2\,e^- \rightarrow HCOO^- + OH^- \qquad (1)$$

$$CO_2 + H_2O + 2\,e^- \rightarrow CO + 2\,OH^- \qquad (2)$$

$$2\,H_2O + 2\,e^- \rightarrow H_2 + 2\,OH^- \qquad (3)$$

$$2\,H^+ + 2\,e^- \rightarrow H_2 \qquad (4)$$

$$CO_2 + OH^- \rightarrow HCO_3^- \qquad (5)$$
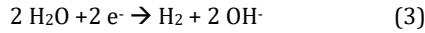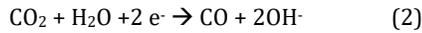
and (2) reactions occurring at the BPM interface:

$$OH^- + H^+ \rightarrow H_2O \qquad (6)$$

$$HCO_3^- + H^+ \rightarrow CO_2 + H_2O \leftrightarrow H_2CO_3 \qquad (7)$$

$$HCOO^- + H^+ \rightarrow HCOOH \qquad (8)$$
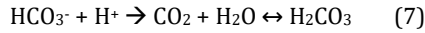
From Eqs. 1 and 2 it is noted that, depending on which eCO2R reaction is dominating, the composition of (ionic) species can differ. If a formate favoring electrocatalyst (e.g. SnO_2) is used, two electrons are consumed, and one hydroxyl ion and one molecule of formate is formed for each consumed CO_2 molecule. If a CO favoring electrocatalyst (e.g. Ag) is used, likewise two electrons are consumed, but two hydroxyl ions instead of one are formed, to produce one molecule CO and to consume one molecule CO_2. This difference in number of electrons to the number of formed hydroxyl ions states a fundamental difference with respect to the pH, as is shown in fig 1.

On the one hand, at the electrode interface, as is shown in literature[59], the formation of hydroxyl ions leads to a local increase in pH, which results in the production of bicarbonate by neutralizing CO_2 (eq.5). On the other hand, at the membrane interface, to uphold the charge balance inside the cell, two protons will be released, creating a local decrease in pH (fig. 2). These protons will react with carbonate, releasing CO_2 (eq. 7).[60]

When producing CO, the total net change of bicarbonate and pH remains zero as the number of produced hydroxyl ions and protons is balanced. During formate production, only one hydroxyl ion is formed per molecule of formate which requires the consumption of two electrons and thus two protons are discharged at the BPM. This imbalance in hydroxyl ions produced versus protons discharged by the BPM results in a net consumption of bulk bicarbonate. Here, the total net change in bicarbonate and pH cannot remain zero but is expected to decrease.
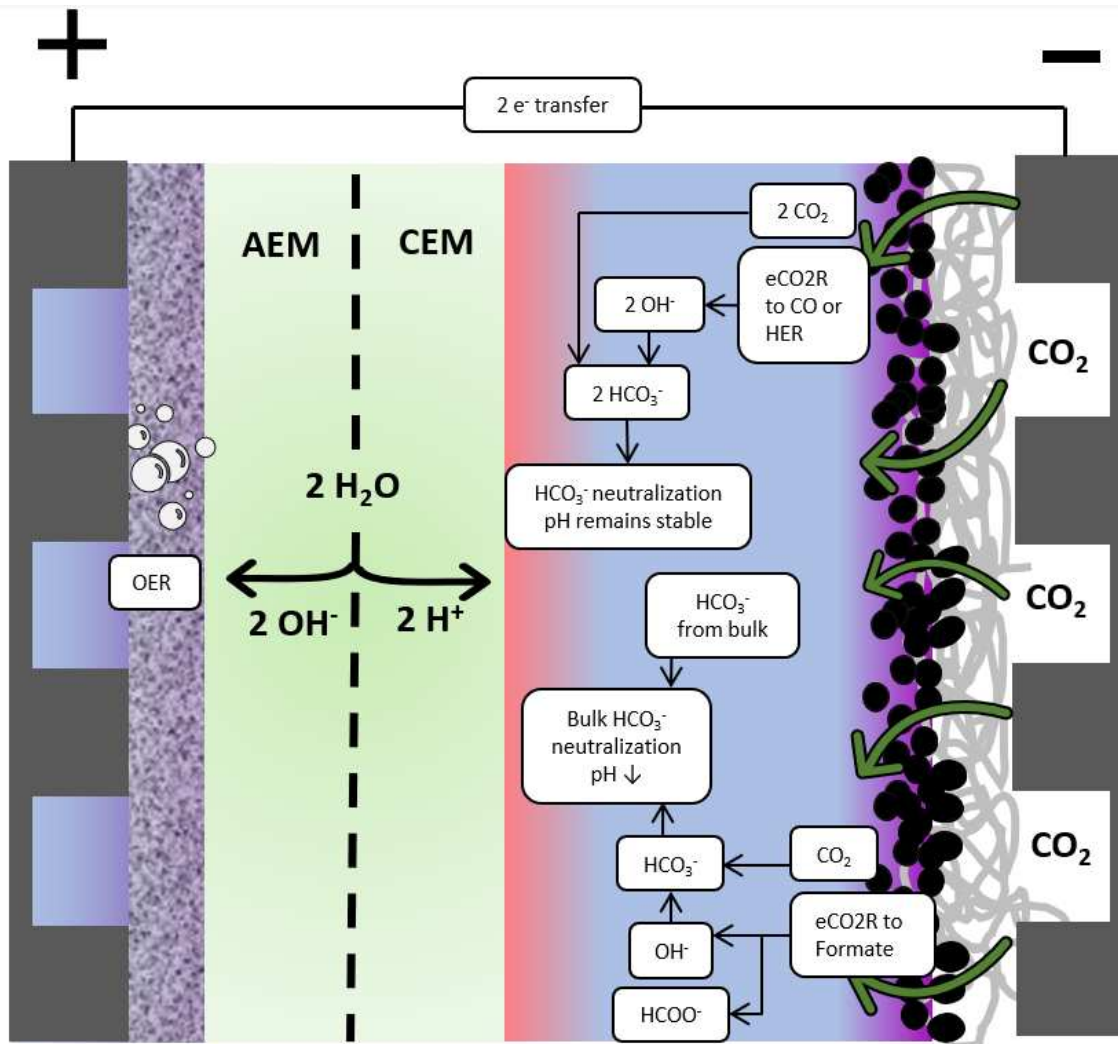
Figure 2. Schematic presentation of the ion movement in BPM based flow-by eCO2R electrolyzers.

At low current densities, the production of formate and hydroxyl ions is rather limited and consequently also the consumption of bulk bicarbonate. As a result, the buffering characteristics of the CO_2/HCO_3^- equilibrium will mask the pH effects at the cost of its own depletion. However at industrial relevant current densities (> 100mA/cm^2) one will reach a point where the buffer can no longer compensate for the bulk carbonate consumption and the catholyte loses its ability to buffer the excess of protons. At this point all bicarbonate will be converted towards CO_2/H_2CO_3 and the excess of protons will drastically lower the pH. However, in current BPM literature this drop in catholyte bulk pH has not yet been reported. On the contrary, the use of BPM is described as a means to maintain a constant pH gradient between the electrolyte compartments[61], which, as can be deduced from the governing reactions (Eqs. 1-8), is impossible if formate is the targeted product. It is assumed that the pH effect is masked by high catholyte flow rates, rapidly refreshing the consumed HCO_3^- ions and thereby stabilizing the pH. This, however, comes at the cost of a diluted product stream and consequently resulting in an increased downstream processing cost.

Influence of $J_{Formate}$ on the catholyte pH

The behavior of BPMs was investigated using the electrolyzer in flow-by configuration, of which the lay-out is discussed in detail in the experimental section. The flowrate of the catholyte was set at 1 ml/min. The data obtained with either a SnO$_2$ or Ag spray-coated GDE are presented in figure 3 (a-d). Sn based electrocatalysts are known to be highly selective towards formate.[62] Nonetheless, at low current densities (< 25 mA/cm^2), when the cell voltage is minimal, besides formate, of which the Faradaic efficiency (FE) was 62%, also a large fraction of CO (36%) is produced (figure 3 (a)). This can be ascribed to the lower Nernst potential of CO production (-0.103 V vs SHE) in contrast with formate production (-0.199 V vs SHE). By increasing the current density, the cell voltage rose and thereby the selectivity of
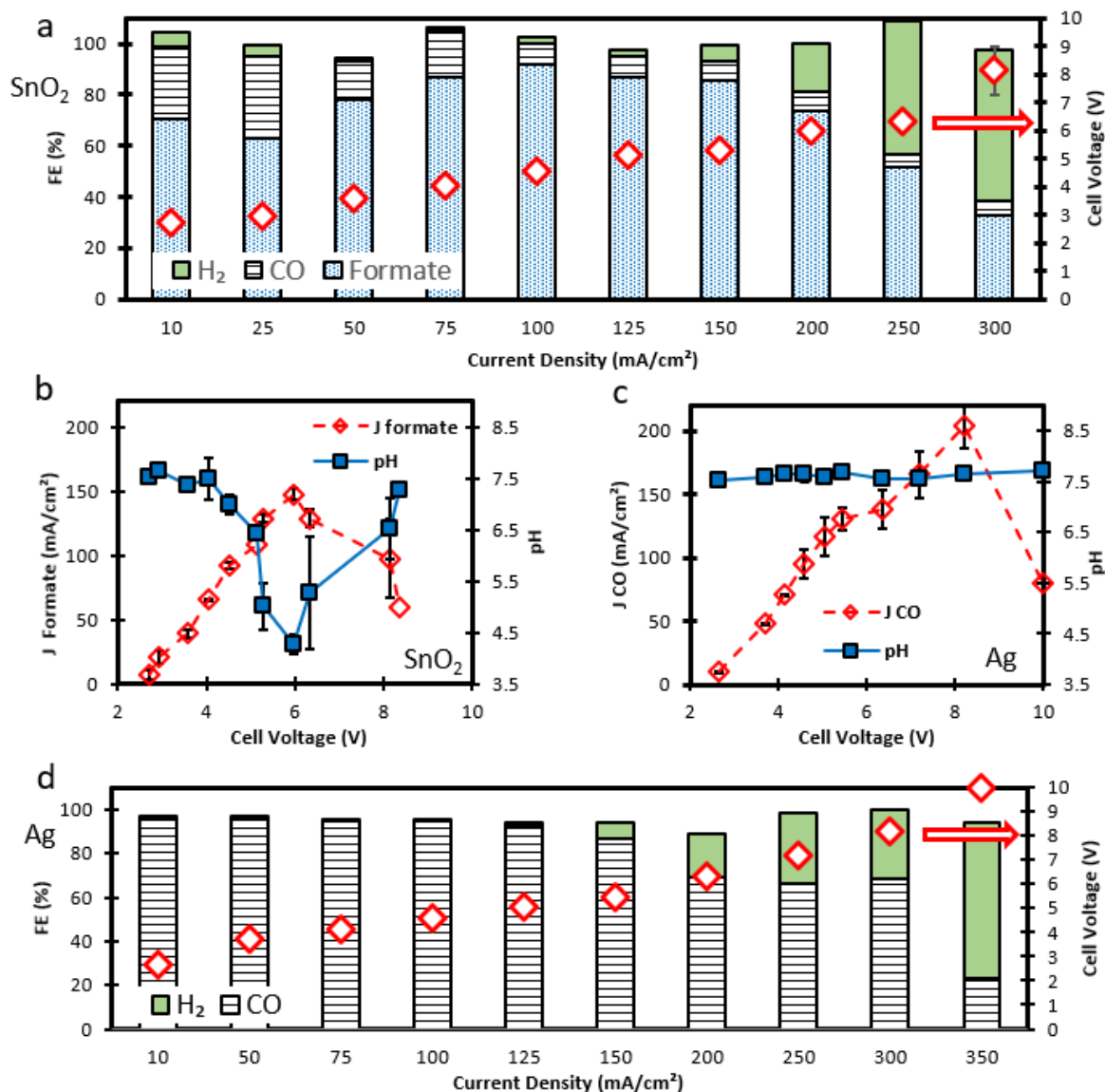
Figure 3. (a) FE (%) and cell voltage (V) plotted versus the applied current density for a CO_2 flow-by electrolyzer with a SnO_2 coated GDE (2.5 mg/cm² and 15% Nafion binder). The catholyte (0.5 M $KHCO_3$) flowrate was set at 1 ml/min, the anolyte flowrate (2 M KOH) at 20 ml/min and the CO_2 flowrate at 200 ml/min. (b) Partial polarization curve of the eCO2R towards formate on SnO_2 particles and (c) towards CO on Ag particles. Bulk pH of the catholyte is plotted on the secondary y-axis. (d) FE (%) and cell voltage (V) plotted versus the applied current density for a CO_2 flow-by electrolyzer with an Ag coated GDE (2.5 mg/cm² and 15% Nafion binder).

the electrolyzer was shifted further towards formate. At 100 mA/cm² the cell reached a maximal formate selectivity of 90%. Upon further increase of the current density, the FE of formate reached a plateau where it remained stable around 80% and more hydrogen was produced. At rising current densities, the amount of hydroxyl ions formed at the catalyst surface and consequently the amount of gaseous CO_2 being neutralized (eq.5) increases as well, limiting the

amount of CO_2 at the three phase boundary. Above 150 mA/cm², the mass transfer of CO_2 towards the catalyst surface is insufficient to continue the eCO2R. Here, the hydrogen evolution reaction (HER) starts to dominate. Since two hydroxyl ions are formed during the HER (eq. 3) the depletion rate of CO_2 at the catalyst surface increases and the partial current density towards formate gradually declines. At the maximum applied current density (300 mA/cm²) the HER accounted for roughly 50% of the total electron consumption. Meanwhile the voltage response of the cell increased linearly with the applied current.

From the theoretical deduction provided above it is clear that, at sufficiently low catholyte flowrates, a drop in pH is expected. To investigate whether this theory is valid, the bulk pH of the catholyte leaving the cell was measured and plotted versus the cell voltage and partial formate current density on figure 3 (b). When the electrolyzer was operated at low total current densities (i.e. 10-75 mA/cm²), corresponding to cell voltages below 4 V, the pH of the electrolyte was stable around 7.3, which

corresponds to the pH of a 0.5M $KHCO_3$ solution saturated with CO_2. The saturation of CO_2 originates from the formation of CO_2 bubbles at the BPM interface, where protons are released and react with bicarbonate (eq. 7).[60] After a threshold partial current density of formate of 60 mA/cm^2 the pH of the catholyte linearly declined to 6.9 at 90 mA/cm^2 and 6.4 at 110 mA/cm^2. It is important to notice that at this latter point the bulk pH of the catholyte was nearly equal to the pKa of the CO_2/HCO_3^- buffer (= 6.1), meaning that the concentration of bicarbonate ions in the catholyte has approximately decreased by 50%, compared to its initial concentration (i.e. 0.5 M). Eventually both the partial current density of formate and the pH reached a peak at 145 mA/cm^2 and 4.3 respectively at a cell voltage of 6 V. From the equilibrium data of the $CO_2/HCO_3^-/CO_3^{2-}$ mixture (figure S1), it can be understood that the fraction of bicarbonate (0.79 %) and carbonate (0.0001%) is negligible at this pH. At higher cell voltages the partial current density of formate declined due to mass transfer limitations of CO_2. As the number of hydroxyl ions formed at the three phase boundary increases with the partial current density, also the consumption of CO_2 into bicarbonate increases, up until the point where there are no longer sufficient CO_2 molecules present for the eCO2R and the partial current density starts to drop. As of this point the HER becomes more dominant and consequently, the ratio of formed hydroxyl ions compared to the number of protons released by the BPM came closer to unity (HER produces two hydroxyl ions as opposed to formate production which produces only one hydroxyl ion) . As a result, the depletion of bulk HCO_3^- is lower, making the pH rise again, eventually up to its original value of 7.3.

To further confirm the expected pH behavior deducted from the governing reactions (Eqs. 1-8), similar tests were conducted, now targeting CO as product of the eCO2R, by utilizing an Ag electrocatalyst. In this case, the total net consumption of bicarbonate is zero, and the pH is expected to remain stable, in contrast to the results acquired with a SnO_2 catalyst. The results from Fig. 3 (c -d) show that the behavior of the Ag catalyst at low current densities (10 – 75 mA/cm^2) were comparable to the SnO_2 catalyst with the only difference being the formed product; CO instead of formate. However, at current densities above 75 mA/cm^2, the catholyte pH with the SnO_2 catalyst drastically decreased, while with the Ag catalyst no such decrease in pH was observed (figure 3 (c)). Even up to partial current densities of CO above 200 mA/cm^2, the pH remained stable at 7.3. Even at high cell voltages (>7 V) where HER starts to dominate and the partial current density of CO reached a peak, the pH remained stable. This is in accordance with the fact that two hydroxyl ions are formed with the formation of a CO molecule (Eq. 2), resulting in a net zero total change of bicarbonate and thus a stable pH. Consequently, these results show that an unstable pH behavior can be ascribed to the production of formate and the imbalance in produced hydroxyl ions and protons, which was so far never discussed in literature.

From these findings, it is now possible to hypothesize the effect other eCO2R products have on the catholyte pH. Firstly, there is a group of gaseous hydrocarbons such as ethyne and methane which are produced mainly on copper based catalyst. For these products, the amount of hydroxyl ions produced during the reaction are matched by the amount of electrons consumed, similar to the production of CO as described above. Here it is logical that the pH will behave similar and therefore will remain constant regardless of the current density and flowrate. Secondly, a group of liquid hydrocarbons, such as methanol, ethanol and acetic acid can also be produced, again typically on a copper based catalyst. Since ethanol and methanol do not dissociate in water, the influence of their production is non-existent. Acetic acid however, does dissociates and therefore theoretically will contribute to a pH decrease similarly to formate. However, in current literature no significant partial current densities towards acetic acid have been published, which is shown to be a key parameter to have significant changes in pH that can be followed experimentally. Thus while theoretically possible, the influence of acetic acid formation on the pH will be difficult to establish experimentally as long as no better catalyst, generating higher currents, is found.

<u>Tuning the formic acid production by altering the catholyte flowrate</u>

As shown above the pH of the catholyte is affected by the partial current density of formate in BPM equipped electrolyzers, presumably also the low flowrate of catholyte had a partial contribution to this observation. Consequently the question rises how this flow rate affects the pH change and if this impacts the cell's performance.

To answer this question, the behavior of the electrolyzer was investigated while varying the flow rate of catholyte between 0.3 ml/min and 5 ml /min (fig 4 (a)). When the cell voltage was kept below 3 V, the influence of the electrolyte flowrate was negligible as all three cases show similar partial current densities and pH. By setting the flowrate to 5 ml/min, the pH of the catholyte remained stable throughout the entire set of experiments. Due to a faster regeneration of catholyte, the buffer was able to withstand the acidic effect of the BPM, thereby masking the depletion of bulk HCO_3^-. Indeed, even at a peak partial current density of 167 mA/cm^2, the pH was still unchanged at 7.3. From literature one would expect that a stable alkaline pH at the cathode side would be beneficial for the reactor performance since a low pH promotes HER. Surprisingly, from the partial polarization curves (see fig. 4 (b)), very little difference in performance was observed between the experiments at 1 ml/min and 5 ml/min. The peak partial current density achieved at 5 ml/min, where the pH remained stable at 7.3, was 167 +/- 7 mA/cm^2 while at 1 ml/min similar partial current densities were achieved (i.e. 150 +/- 5 mA/cm^2) at a pH as low as 4.3. This clearly shows that the cell performance, in terms of peak partial current density, is not necessarily limited by the bulk acidic catholyte environment. This observation is in sheer contrast with literature, where it was assumed that acidic environments are not suitable for eCO2R. However, recently Bonue et al. observed a similar phenomenon in a differential electrochemical mass spectroscopy set-up.[59] Here it was concluded that eCO2R in (bulk) acidic environment is achievable if one can prevent the transport of protons towards the cathode interface, i.e. the pH of the bulk is less important if one can control the pH at the three phase boundary. In our electrolyzer this is achieved in two ways. First, the low flowrate of catholyte limits

the convective mass transfer of protons from the BPM interface towards the GDE. Second, the high current density creates strong local alkaline conditions by producing hydroxyl ions at the three phase boundary.
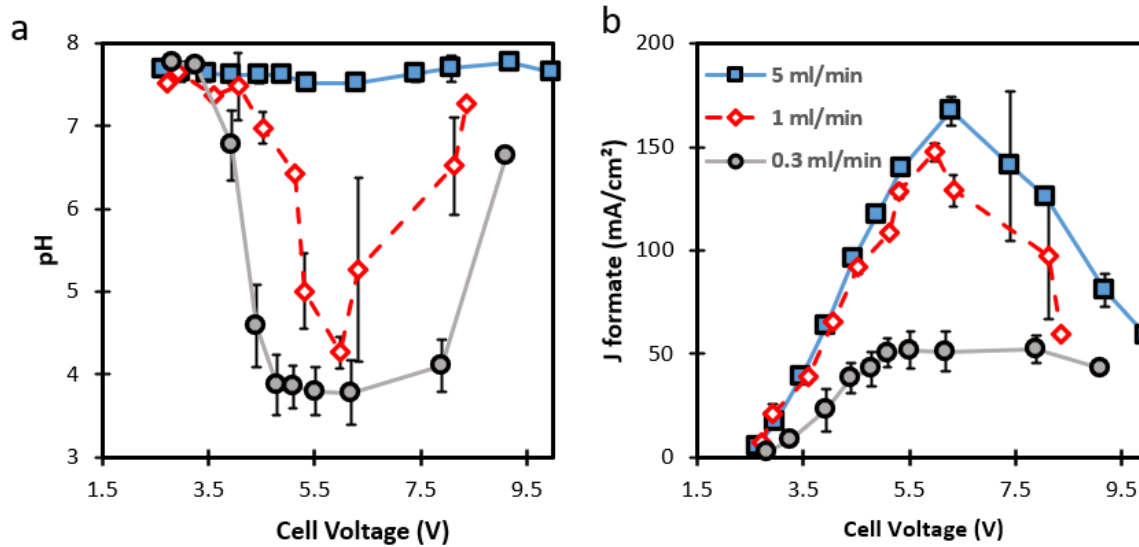

Figure 4. (a) Relation between the catholyte flowrate and its bulk pH of a BPM equipped eCO2R electrolyzer. 5 ml/min (blue, square), 1 ml/min (red, diamond) and 0.3 ml/min (grey, circle). (b) Partial polarization curve for the BPM based eCO2R electrolyzer towards formate /formic acid at a range of catholyte flowrates.

Meanwhile, when the flowrate was set a 0.3 ml/min, the pH drastically declined to 3.7 at cell voltages above 3 V, where it reached a plateau. It makes sense that, due to the lower flowrate (i.e. a lower supply of fresh catholyte) the buffer of the cell is more vulnerable to the excess of protons supplied by the BPM. Interestingly in this case, the low pH does limit the cell performance, since the peak current density at 0.3 ml/min reached a plateau at only 60 mA/cm². Here it can be concluded that the combination of a high amount of protons (low pH of 3.7), the low flow rate and the minimized thickness of the catholyte flow channel can no longer prevent the protons from reaching the GDE through the bulk catholyte chamber and consequently the HER dominates under these conditions. It is essential to understand that the occurrence of a drop in catholyte pH is primarily determined by the selectivity of the eCO2R. As mentioned previously, the pH will remain stable when CO or H_2 are the targeted products, During these reactions the flowrate will have no effect on the pH since here the protons supplied by the BPM are in balance with the hydroxyl ions formed during the eCO2R. Only when formate is targeted, a deficit in bicarbonate occurs which initiates the pH change, after which lowering or increasing the flowrate can respectively further promote this pH drop or inhibit it.

Furthermore, flowrate does not only influence pH and FE but also the concentration of the final product. From figure 5, it can be seen that an increase in flowrate to 5 ml/min, resulted in a limited maximum product concentration of 6.2 g/l at a cell voltage of 6.9 V.
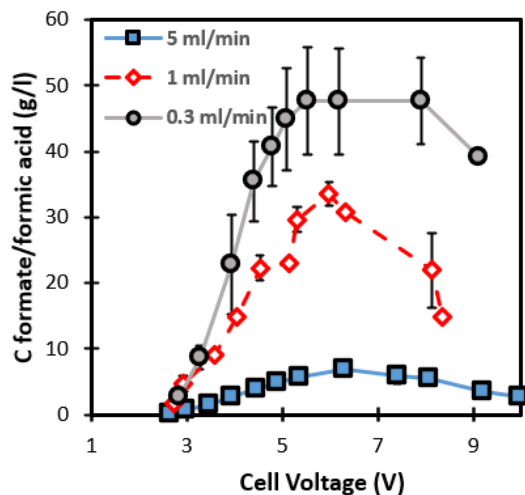
Figure 5. Concertation of formate/formic acid in the catholyte exiting the BPM based eCO2R electrolyzer at different flowrates. 5 ml/min (blue, square), 1 ml/min (red, diamond) and 0.3 ml/min (grey, circle).

By lowering the flowrate to 0.3 ml/min the product is less diluted by the catholyte and thereby concentrations up to 47 g/l were achieved in a cell voltage range of 5.5 V to 7.9 V. Additionally, it can be calculated from known data of the formate/formic acid equilibrium that, due to the low pH of these samples, the formic acid/formate ratio in the final product is 1, showing the benefits of both the low flow rate with respect to downstream processing (higher product concentration) and the low pH on the product distribution. Indeed, for industry formic acid is a more desired product than formate (*vide infra*).
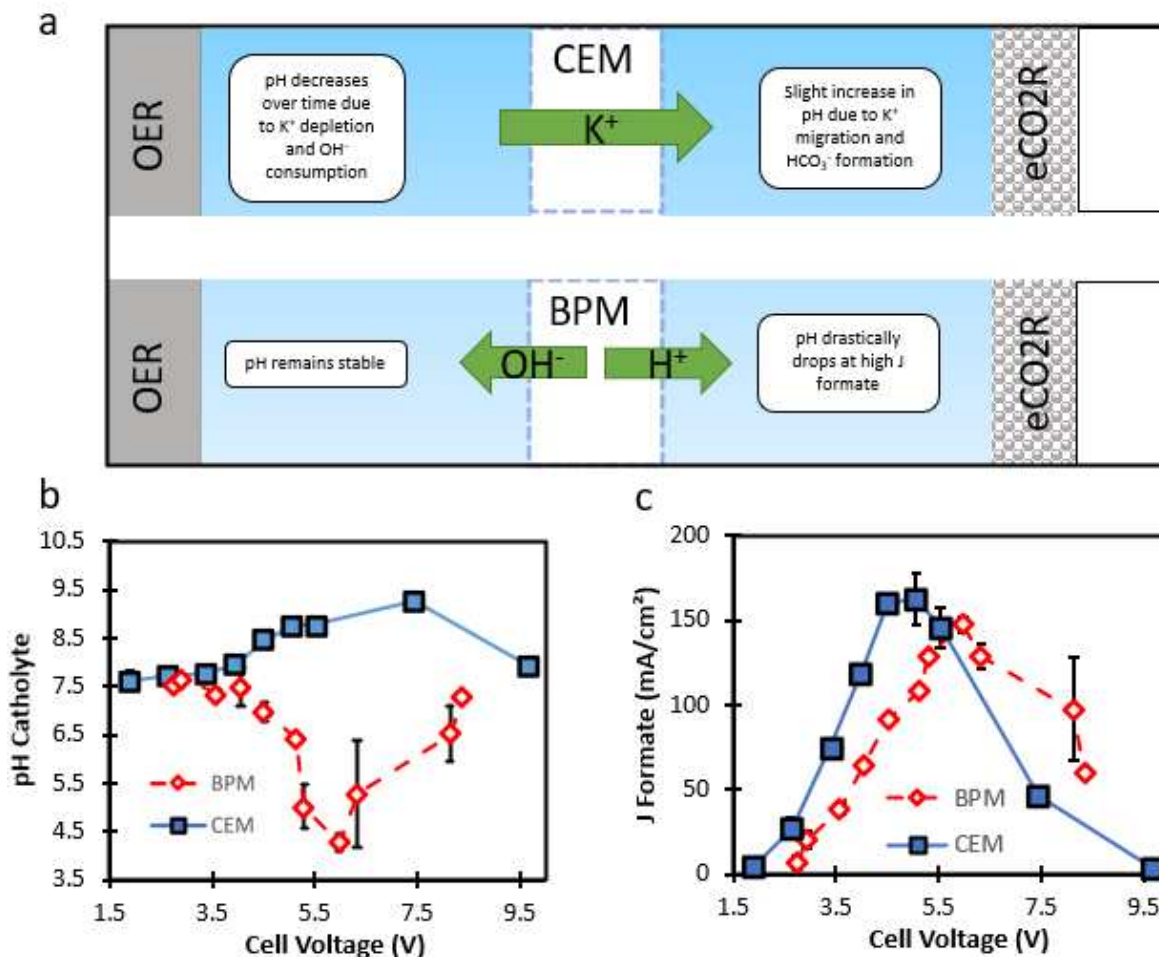

Figure 6: (a) influence of cell voltage on the pH of the bulk catholyte exiting the electrolyzer for a CEM (blue, solid) and a BPM (red, dotted) equipped eCO2R electrolyzer. The Flowrate of catholyte is set at 1 ml/min 0.5M KHCO₃. (b) Partial polarization curve for the eCO2R towards formate/formic acid, both for a CEM and BPM base electrolyzer. (c) ion migration in the electrolyzers and their influence on the electrolyte compartments.

An optimal flowrate was found at 1 ml/min where high product concentrations were achieved (34 g/l) without restraining the cell performance (higher FE's than with 0.3 ml/min). Similar to the samples obtained at 0.3 ml/min the low pH (4.2) at the optimal cell voltage of 6.0 V resulted in a formic acid/formate ratio of 0.67. At this point, it is important to note that it is the first time that with a BPM equipped eCO2R electrolyzer formic acid rather than formate is produced at such high concentrations. Since the conversion of formate to formic acid requires an additional downstream process, the direct formation of formic acid is industrially more interesting. Therefore these findings are of great importance for the eCO2R research society.

J_formate at constant pH

Finally, the behavior of a BPM equipped electrolyzer is compared to a cation exchange membrane (CEM) equipped electrolyzer. In this case Nafion 117 is used, which can be regarded as the benchmark membrane for eCO2R reactor engineering. From a theoretical perspective, it can be understood that the migration of ionic species will be completely different for both cases. Due to an excess of potassium ions in the 2 M KOH anolyte, the cations migrating through the CEM will be potassium rather than protons, in contrast to the BPM, where protons are released in the catholyte (Fig. 6 (a)).[50] As a result, no protons

are supplied at the cathode side of the CEM, thereby the consumption of bicarbonate will be non-existent, even when the partial current density of formate is high. Consequently, during the CEM electrolyzer experiments, the bulk pH of the catholyte remained alkaline over the entire range of measured current densities, figure 6 (b). In fact, due to the formation of bicarbonate at the GDE interface (eq. 5), the pH slightly rose towards 9.5.

Since the maximum partial current density for the two membranes were almost identical while the pH differed up to 4.5 units, figure 6 (c), it can be concluded that the low pH obtained with the BPM does not necessarily limit the cell performance.

Additionally, on fig 6 (c), at low current densities a 0.8 V shift in cell voltage was observed between the two membranes. This is mainly due the supplementary energy required for the water dissociation at the center junction of the BPM. At higher current densities the shift in cell voltage rose to 1 V, mainly due to the increased ohmic resistance of the BPM compared to the CEM. At present, the increased ohmic resistance is one of the main drawbacks in the application of BPMs, therefore lots of effort is being put in the optimization of BPMs. For example, by creating 3D electro spun junction at the center of the BPM or improved water splitting catalyst, these might allow for better performance in the future. However, the BPM shows a clear advantage over CEMs as it allows to produce formic acid, rather than formate at comparable rates.

CONCLUSIONS

In literature BPM equipped electrolyzers are praised for their high resistance to product crossover and their ability to stabilize a pH gradient in the different reactor compartments. In this work the behavior of these electrolyzers was investigated at low catholyte flow rates to further evaluate these claims. It was found that when formate is the main product, the bulk pH of the catholyte severely decreased at increasing formate partial current densities and decreasing catholyte flow rates. When CO formation is favored, this effect is absent, which is in accordance with the governing reactions. Indeed it can be understood from the different reactions occurring in the cathode compartment, that due to an excess of protons supplied by the BPM, the buffering capacity of the catholyte is nullified during formate production at high reaction rates. Consequently, the bulk pH of the catholyte decreases. Meanwhile when CO is produced, the protons released by the BPM are neutralized by an equal amount of hydroxyl ions produced during eCO2R, resulting in no net change in pH.

Next, the influence of the flowrate was further investigated by varying it between 0.3; 1 and 5 ml/min, as a point of reference, Chen et al. used 40 ml/min for a 25 cm^2 GDE.[55] At the highest flowrate, the catholyte was refreshed vigorously which prevented the breakdown of the buffer capacity, keeping the pH constant. Surprisingly, the performance of the electrolyzer was almost identical at 5 ml/min and 1 ml/min while the pH in the latter reached values as low as 4.3, meaning that the low pH observed in the BPM electrolyzer does not necessarily limit the cell performance. This is mainly ascribed to the prevention of protons reaching the catalyst surface by slow diffusion and high local alkalinity at the three phase boundary. At the lowest flow rate a strong decrease in reactor performance was noted. At this flowrate the pH of the catholyte was well below 4 and consequently it was no longer possible to prevent protons from reaching the catalyst surface, due to a combination of high proton concentration (low pH) and long residence time in the electrolyzer (low flowrate). An ideal flowrate was found at 1 ml/min, as at this flow rate the protons were not able to reach the catalyst surface, despite the low pH. Consequently, the low pH did not affect the reactor performance and a product concentration up to 34 g/L was obtained. Moreover, due to the low bulk pH almost half of the liquid produced was formic acid rather than formate, which is very rarely reported in literature. It is important to notice that while the flowrate affects the pH change in the catholyte it is still the product selectivity that determines if a pH change occurs or not. Indeed, a change in catholyte pH will not occur when the product selectivity is shifted towards CO or hydrogen, regardless of the flow rate, since here no consumption of the buffer takes place.

Finally the behavior of pH at 1 ml/min was compared to a CEM equipped electrolyzer. Here, due to the migration of potassium rather than protons, the net pH of the catholyte compartment even slightly increased. Once again, the performance of the CEM electrolyzer was found to be almost identical to the BPM electrolyzer, regardless of the immense difference in pH. This shows again that acidic bulk pH does not necessarily limit the cell performance.

Overall it is clear that BPMs show great potential use in eCO2R electrolyzers. Yet, for the implementation of this reactor design on an industrial scale additional steps need to be taken. More specifically future work should be focused on optimizing the performance by reducing the high voltage drop across the membrane and improves its water uptake in order to increase the stability at high current densities. Furthermore it is essential that these newly developed BPMs become commercially available to implement them in the next generation CO_2 electrolyzers. Meanwhile, in this work, an ideal flowrate in terms of performance, product concentration and formic acid ratio, was obtained, allowing to operate eCO2R electrolyzers under acidic environment, considered a holy grail in formic acid production.

AUTHOR INFORMATION

Corresponding Author

* Tom Breugelmans: Tom.breugelmans@uantwerpen.be

Author Contributions

The manuscript was written through contributions of all authors.

ACKNOWLEDGMENT

ABBREVIATIONS

CCU, Carbon Capture & Utilization; CO_2, Carbon Dioxide; eCO2R, electrochemical CO_2 reduction; GDE; gas diffusion electrode; CEM, cation exchange membrane; AEM anion exchange membrane; BPM, bipolar membrane; FE, Faradaic efficiency; HER, hydrogen evolution reaction

REFERENCES

[1]   M. Aresta, Carbon Dioxide: Utilization Options to Reduce its Accumulation in the Atmosphere, in: Carbon Dioxide as Chem. Feed., Wiley-VCH, 2010: pp. 1–13. doi:10.1002/9783527629916.ch1.

[2]   M. Aresta, A. Dibenedetto, Utilisation of CO2 as a chemical feedstock: Opportunities and challenges, J. Chem. Soc. Dalt. Trans. (2007) 2975–2992. doi:10.1039/b700658f.

[3]   R. Masel, Z. Liu, D. Zhao, Q. Chen, D. Lutz, L. Nereng, CO2 conversion to chemicals with emphasis on using renewable energy/resources to drive the conversion, in: RSC Green Chem., Royal Society of Chemistry, 2016: pp. 215–257. doi:10.1039/9781782622444-00215.

[4]   O.S. Bushuyev, P. De Luna, C.T. Dinh, L. Tao, G. Saur, J. van de Lagemaat, S.O. Kelley, E.H. Sargent, What Should We Make with CO2 and How Can We Make It?, Joule. 2 (2018) 825–832. doi:10.1016/j.joule.2017.09.003.

[5]   D.T. Whipple, P.J.A. Kenis, Prospects of CO2 utilization via direct heterogeneous electrochemical reduction, J. Phys. Chem. Lett. 1 (2010) 3451–3458. doi:10.1021/jz1012627.

[6]   O.G. Sánchez, Y.Y. Birdja, M. Bulut, J. Vaes, T. Breugelmans, D. Pant, Recent advances in industrial CO2 electroreduction, Curr. Opin. Green Sustain. Chem. (2019). doi:10.1016/J.COGSC.2019.01.005.

[7]   N. Daems, B. De Mot, D. Choukroun, K. Van Daele, C. Li, A. Hubin, S. Bals, J. Hereijgers, T. Breugelmans, Nickel-containing N-doped carbon as effective electrocatalysts for the reduction of CO2 to CO in a continuous-flow electrolyzer, Sustain. Energy Fuels. 4 (2020) 1296–1311. doi:10.1039/c9se00814d.

[8]   J. Choi, M.J. Kim, S.H. Ahn, I. Choi, J.H. Jang, Y.S. Ham, J.J. Kim, S.K. Kim, Electrochemical CO2 reduction to CO on dendritic Ag-Cu electrocatalysts prepared by electrodeposition, Chem. Eng. J. 299 (2016) 37–44. doi:10.1016/j.cej.2016.04.037.

[9]   H. Li, N. Xiao, M. Hao, X. Song, Y. Wang, Y. Ji, C. Liu, C. Li, Z. Guo, F. Zhang, J. Qiu, Efficient CO2 electroreduction over pyridinic-N active sites highly exposed on wrinkled porous carbon nanosheets, Chem. Eng. J. 351 (2018) 613–621. doi:10.1016/j.cej.2018.06.077.

[10]   J. Albo, G. Beobide, P. Castaño, A. Irabien, Methanol electrosynthesis from CO2at Cu2O/ZnO prompted by pyridine-based aqueous solutions, J. CO2 Util. 18 (2017) 164–172. doi:10.1016/j.jcou.2017.02.003.

[11]   J. Albo, A. Irabien, Cu2O-loaded gas diffusion electrodes for the continuous electrochemical reduction of CO2 to methanol, J. Catal. 343 (2016) 232–239. doi:10.1016/j.jcat.2015.11.014.

[12]   C. Dinh, T. Burdyny, G. Kibria, A. Seifitokaldani, C.M. Gabardo, F.P.G. de Arquer, A. Kiani, J.P. Edwards, P. De Luna, O.S. Bushuyev, C. Zou, R. Quintero-Bermudez, Y. Pang, D. Sinton, E.H. Sargent, Sustained high-selectivity CO 2 electroreduction to ethylene via hydroxide-mediated catalysis at an abrupt reaction interface. Submitted to, Science (80-.). 787 (2018) 783–787. doi:10.1126/science.aas9100.

[13]   M. Rumayor, A. Dominguez-Ramos, P. Perez, A. Irabien, A techno-economic evaluation approach to the electrochemical reduction of CO2 for formic acid manufacture, J. CO2 Util. 34 (2019) 490–499. doi:10.1016/j.jcou.2019.07.024.

[14]   A.S. Agarwal, Y. Zhai, D. Hill, N. Sridhar, The electrochemical reduction of carbon dioxide to formate/formic acid: Engineering and economic feasibility, ChemSusChem. 4 (2011) 1301–1310. doi:10.1002/cssc.201100220.

[15]   F. Bienen, D. Kopljar, A. Löwe, P. Aßmann, M. Stoll, P. Rößner, N. Wagner, A. Friedrich, E. Klemm, Utilizing Formate as an Energy Carrier by Coupling CO2 Electrolysis with Fuel Cell Devices, Chemie-Ingenieur-Technik. 91 (2019) 872–882. doi:10.1002/cite.201800212.

[16]   S. Zhang, P. Kang, T.J. Meyer, Nanostructured tin catalysts for selective electrochemical reduction of carbon dioxide to formate, J. Am. Chem. Soc. 136 (2014) 1734–1737. doi:10.1021/ja4113885.

[17]   C. Zhao, J. Wang, Electrochemical reduction of CO2 to formate in aqueous solution using electro-deposited Sn catalysts, Chem. Eng. J. 293 (2016) 161–170. doi:10.1016/j.cej.2016.02.084.

[18]   Q. Yang, Q. Wu, Y. Liu, S. Luo, X. Wu, X. Zhao, H. Zou, B. Long, W. Chen, Y. Liao, L. Li, P.K. Shen, L. Duan, Z. Quan, Novel Bi-Doped Amorphous SnO $_x$ Nanoshells for Efficient Electrochemical CO $_2$ Reduction into Formate at Low Overpotentials, Adv. Mater. 32 (2020) 2002822. doi:10.1002/adma.202002822.

[19]   S. Sen, S.M. Brown, M.L. Leonard, F.R. Brushett, Electroreduction of carbon dioxide to formate at high current densities using tin and tin oxide gas diffusion electrodes, J. Appl. Electrochem. 49 (2019) 917–928. doi:10.1007/s10800-019-01332-z.

[20]   S. Lee, J.D. Ocon, Y. Il Son, J. Lee, Alkaline CO2 electrolysis toward selective and continuous HCOO- production over SnO2 nanocatalysts, J. Phys. Chem. C. 119 (2015) 4884–4890. doi:10.1021/jp512436w.

[21]   G. Wen, D.U. Lee, B. Ren, F.M. Hassan, G. Jiang, Z.P. Cano, J. Gostick, E. Croiset, Z. Bai, L. Yang, Z. Chen, Orbital Interactions in Bi-Sn Bimetallic Electrocatalysts for Highly Selective Electrochemical CO $_2$ Reduction toward Formate Production, Adv. Energy Mater. 8 (2018) 1802427. doi:10.1002/aenm.201802427.

[22]   K. Fan, Y. Jia, Y. Ji, P. Kuang, B. Zhu, X. Liu, J. Yu, Curved Surface Boosts Electrochemical CO2 Reduction to Formate via Bismuth Nanotubes in a Wide Potential Window, ACS Catal. 10 (2020) 358–364. doi:10.1021/acscatal.9b04516.

[23]   B. Bohlen, D. Wastl, J. Radomski, V. Sieber, L. Vieira, Electrochemical CO2 reduction to formate on indium catalysts prepared by electrodeposition in deep eutectic solvents, Electrochem. Commun. 110 (2020) 106597. doi:10.1016/j.elecom.2019.106597.

[24]   R. Hegner, L.F.M. Rosa, F. Harnisch, Electrochemical CO2 reduction to formate at indium electrodes with high efficiency and selectivity in pH neutral electrolytes, Appl. Catal. B Environ. 238 (2018) 546–556. doi:10.1016/j.apcatb.2018.07.030.

[25]   P. Deng, F. Yang, Z. Wang, S. Chen, Y. Zhou, S. Zaman, B.Y. Xia, Metal–Organic Framework-Derived Carbon Nanorods Encapsulating Bismuth Oxides for Rapid and Selective CO $_2$ Electroreduction to Formate, Angew. Chemie Int. Ed. 59 (2020) 10807–10813. doi:10.1002/anie.202000657.

[26] F. Li, G.H. Gu, C. Choi, P. Kolla, S. Hong, T.S. Wu, Y.L. Soo, J. Masa, S. Mukerjee, Y. Jung, J. Qiu, Z. Sun, Highly stable two-dimensional bismuth metal-organic frameworks for efficient electrochemical reduction of CO2, Appl. Catal. B Environ. 277 (2020) 119241. doi:10.1016/j.apcatb.2020.119241.

[27] J.X. Wu, S.Z. Hou, X. Da Zhang, M. Xu, H.F. Yang, P.S. Cao, Z.Y. Gu, Cathodized copper porphyrin metal-organic framework nanosheets for selective formate and acetate production from CO2 electroreduction, Chem. Sci. 10 (2019) 2199–2205. doi:10.1039/c8sc04344b.

[28] J. Wang, H. Wang, Z. Han, J. Han, Electrodeposited porous Pb electrode with improved electrocatalytic performance for the electroreduction of CO2 to formic acid, Front. Chem. Sci. Eng. 9 (2015) 57–63. doi:10.1007/s11705-014-1444-8.

[29] S. Back, J.H. Kim, Y.T. Kim, Y. Jung, On the mechanism of high product selectivity for HCOOH using Pb in CO2 electroreduction, Phys. Chem. Chem. Phys. 18 (2016) 9652–9657. doi:10.1039/c6cp00542j.

[30] C.X. Zhao, Y.F. Bu, W. Gao, Q. Jiang, CO2 Reduction Mechanism on the Pb(111) Surface: Effect of Solvent and Cations, J. Phys. Chem. C. 121 (2017) 19767–19773. doi:10.1021/acs.jpcc.7b04375.

[31] B. Endrődi, G. Bencsik, F. Darvas, R. Jones, K. Rajeshwar, C. Janáky, Continuous-flow electroreduction of carbon dioxide, Prog. Energy Combust. Sci. 62 (2017) 133–154. doi:10.1016/J.PECS.2017.05.005.

[32] T. Burdyny, W.A. Smith, CO2 reduction on gas-diffusion electrodes and why catalytic performance must be assessed at commercially-relevant conditions, Energy Environ. Sci. 12 (2019) 1442–1453. doi:10.1039/c8ee03134g.

[33] S. Verma, B. Kim, H.R.M. Jhong, S. Ma, P.J.A. Kenis, A gross-margin model for defining technoeconomic benchmarks in the electroreduction of CO2, ChemSusChem. 9 (2016) 1972–1979. doi:10.1002/cssc.201600394.

[34] J. Song, H. Song, B. Kim, J. Oh, Towards Higher Rate Electrochemical CO2 Conversion: From Liquid-Phase to Gas-Phase Systems, Catalysts. 9 (2019) 224. doi:10.3390/catal9030224.

[35] C. Delacourt, P.L. Ridgway, J.B. Kerr, J. Newman, Design of an electrochemical cell making syngas (CO+ H2) from C O2 and H2 O reduction at room temperature, J. Electrochem. Soc. 155 (2008). doi:10.1149/1.2801871.

[36] H. Xiang, H.A. Miller, M. Bellini, H. Christensen, K. Scott, S. Rasul, E.H. Yu, Production of formate by CO2 electrochemical reduction and its application in energy storage, Sustain. Energy Fuels. 4 (2019) 277–284. doi:10.1039/c9se00625g.

[37] D. Kopljar, A. Inan, P. Vindayer, N. Wagner, E. Klemm, Electrochemical reduction of CO2 to formate at high current density using gas diffusion electrodes, J. Appl. Electrochem. 44 (2014) 1107–1116. doi:10.1007/s10800-014-0731-x.

[38] E. Irtem, T. Andreu, A. Parra, M.D. Hernández-Alonso, S. García-Rodríguez, J.M. Riesco-García, G. Penelas-Pérez, J.R. Morante, Low-energy formate production from CO2 electroreduction using electrodeposited tin on GDE, J. Mater. Chem. A. 4 (2016) 13582–13588. doi:10.1039/c6ta04432h.

[39] J.-B. Vennekoetter, R. Sengpiel, M. Wessling, Beyond the catalyst: How electrode and reactor design determine the product spectrum during electrochemical CO2 reduction, Chem. Eng. J. 364 (2019) 89–101. doi:10.1016/J.CEJ.2019.01.045.

[40] A. Del Castillo, M. Alvarez-Guerra, J. Solla-Gullón, A. Sáez, V. Montiel, A. Irabien, Electrocatalytic reduction of CO2 to formate using particulate Sn electrodes: Effect of metal loading and particle size, Appl. Energy. 157 (2015) 165–173. doi:10.1016/j.apenergy.2015.08.012.

[41] B. De Mot, J. Hereijgers, M. Duarte, T. Breugelmans, Influence of flow and pressure distribution inside a gas diffusion electrode on the performance of a flow-by CO2 electrolyzer, Chem. Eng. J. 378 (2019) 122224. doi:10.1016/j.cej.2019.122224.

[42] M. Leonard, L.E. Clarke, A. Forner-Cuenca, S.M. Brown, F. Brushett, Investigating Electrode Flooding in a Flowing Electrolyte, Gas-Fed Carbon Dioxide Electrolyzer, ChemSusChem. (2019) cssc.201902547. doi:10.1002/cssc.201902547.

[43] G. Díaz-Sainz, M. Alvarez-Guerra, B. Ávila-Bolívar, J. Solla-Gullón, V. Montiel, A. Irabien, Improving trade-offs in the figures of merit of gas-phase single-pass continuous CO2 electrocatalytic reduction to formate, Chem. Eng. J. 405 (2021) 126965. doi:10.1016/j.cej.2020.126965.

[44] M. Duarte, B. De Mot, J. Hereijgers, T. Breugelmans, Electrochemical Reduction of CO2: Effect of Convective CO2 Supply in Gas Diffusion Electrodes, ChemElectroChem. 6 (2019) 5596–5602. doi:10.1002/celc.201901454.

[45] T. Lei, X. Zhang, J. Jung, Y. Cai, X. Hou, Q. Zhang, J. Qiao, Continuous electroreduction of carbon dioxide to formate on Tin nanoelectrode using alkaline membrane cell configuration in aqueous medium, Catal. Today. 318 (2018) 32–38. doi:10.1016/j.cattod.2017.10.003.

[46] D.A. Salvatore, D.M. Weekes, J. He, K.E. Dettelbach, Y.C. Li, T.E. Mallouk, C.P. Berlinguette, Electrolysis of Gaseous CO2 to CO in a Flow Cell with a Bipolar Membrane, ACS Energy Lett. 3 (2018) 149–154. doi:10.1021/acsenergylett.7b01017.

[47] D.A. Vermaas, W.A. Smith, Synergistic Electrochemical CO2 Reduction and Water Oxidation with a Bipolar Membrane, ACS Energy Lett. 1 (2016) 1143–1148. doi:10.1021/acsenergylett.6b00557.

[48] M. Ramdin, A.R.T. Morrison, M. De Groen, R. Van Haperen, R. De Kler, L.J.P. Van Den Broeke, J.P. Martin Trusler, W. De Jong, T.J.H. Vlugt, High Pressure Electrochemical Reduction of CO2 to Formic Acid/Formate: A Comparison between Bipolar Membranes and Cation Exchange Membranes, Ind. Eng. Chem. Res. 58 (2019) 1834–1847. doi:10.1021/acs.iecr.8b04944.

[49] C.Y. Liu, C.C. Sung, A review of the performance and analysis of proton exchange membrane fuel cell membrane electrode assemblies, J. Power Sources. 220 (2012) 348–353. doi:10.1016/j.jpowsour.2012.07.090.

[50] B. De Mot, M. Ramdin, J. Hereijgers, T.J.H. Vlugt, T. Breugelmans, Direct Water Injection in Catholyte-Free Zero-Gap Carbon Dioxide Electrolyzers, ChemElectroChem. 7 (2020) 3839–3843. doi:10.1002/celc.202000961.

[51] M. Ma, E.L. Clark, K.T. Therkildsen, S. Dalsgaard, I. Chorkendorff, B. Seger, Insights into the carbon balance for CO2 electroreduction on Cu using gas diffusion electrode reactor designs, Energy Environ. Sci. 13 (2020) 977–985. doi:10.1039/d0ee00047g.

[52] D.A. Vermaas, W.A. Smith, Chapter 8. Applications of Bipolar Membranes for Electrochemical and Photoelectrochemical Water Splitting, in: 2018: pp. 208–238. doi:10.1039/9781782629863-00208.

[53] Y.C. Li, Z. Yan, J. Hitt, R. Wycisk, P.N. Pintauro, T.E. Mallouk, Bipolar Membranes Inhibit Product Crossover in CO2 Electrolysis Cells, Adv. Sustain. Syst. 2 (2018) 1700187. doi:10.1002/adsu.201700187.

[54] N. Wang, R.K. Miao, G. Lee, A. Vomiero, D. Sinton, A.H. Ip, H. Liang, E.H. Sargent, Suppressing the liquid product crossover in electrochemical CO2 reduction, SmartMat. 2 (2021) 12–16. doi:10.1002/smm2.1018.

[55] Y. Chen, A. Vise, W.E. Klein, F.C. Cetinbas, D.J. Myers, W.A. Smith, W.A. Smith, W.A. Smith, T.G. Deutsch, K.C. Neyerlin, A Robust, Scalable Platform for the Electrochemical Conversion of CO2 to Formate: Identifying Pathways to Higher Energy Efficiencies, ACS Energy Lett. 5 (2020) 1825–1833. doi:10.1021/acsenergylett.0c00860.

[56] C. Shen, R. Wycisk, P.N. Pintauro, High performance electrospun bipolar membrane with a 3D junction, Energy Environ. Sci. 10 (2017) 1435–1442. doi:10.1039/c7ee00345e.

[57] S.Z. Oener, L.P. Twight, G.A. Lindquist, S.W. Boettcher, Thin Cation-Exchange Layers Enable High-Current-Density Bipolar Membrane Electrolyzers via Improved Water Transport, ACS Energy Lett. 6 (2021) 1–8. doi:10.1021/acsenergylett.0c02078.

[58] Z. Yan, J.L. Hitt, Z. Zeng, M.A. Hickner, T.E. Mallouk, Improving the efficiency of CO2 electrolysis by using a bipolar membrane with a weak-acid cation exchange layer, Nat. Chem. 13 (2021) 33–40. doi:10.1038/s41557-020-00602-0.

[59] C.J. Bondue, M. Graf, A. Goyal, M.T.M. Koper, Suppression of Hydrogen Evolution in Acidic Electrolytes by Electrochemical CO2 Reduction, J. Am. Chem. Soc. 143 (2021) 279–285. doi:10.1021/jacs.0c10397.

[60] T. Li, E.W. Lees, M. Goldman, D.A. Salvatore, D.M. Weekes, C.P. Berlinguette, Electrolytic Conversion of Bicarbonate into CO in a Flow Cell, Joule. 3 (2019) 1487–1497. doi:10.1016/j.joule.2019.05.021.

[61]   Y.C. Li, D. Zhou, Z. Yan, R.H. Gonçalves, D.A. Salvatore, C.P. Berlinguette, T.E. Mallouk, Electrolysis of CO2 to Syngas in Bipolar Membrane-Based Electrochemical Cells, ACS Energy Lett. 1 (2016) 1149–1153. doi:10.1021/acsenergylett.6b00475.

[62]   A. Del Castillo, M. Alvarez-Guerra, A. Irabien, Continuous electroreduction of CO $_2$ to formate using Sn gas diffusion electrodes, AIChE J. 60 (2014) 3557–3564. doi:10.1002/aic.14544.

Electrochemical CO_2 reduction in BPM electrolyzers